

A Large Scale 3D Global Full Particle Simulation of the Solar Wind-Terrestrial Magnetosphere Interaction for Bepi Colombo Mercury Exploration

Project Representative

Dongsheng Cai

Faculty of Engineering, Information and Systems, University of Tsukuba

Author

Dongsheng Cai

Faculty of Engineering, Information and Systems, University of Tsukuba

In the present paper, to our knowledge, the first 3D global full electro-magnetic particle simulation in the global view of solar-wind-magnetosphere interaction are performed, and compared with the statistical surveys of the plasma flows measured by the Cluster spacecraft in the high-altitude cusp region of the Northern Hemisphere. The magnetospheric polar cusp regions are considered to be key regions to transfer mass, and energy from the solar-wind to the plasma sheet. Using the global PIC simulation, we try to understand these key regions and the dynamical interactions that occur there. The basic structures of the so-called stagnant cusp exterior (SEC) are observed in the simulation. The sub-Alfvénic layers which consider to be the plasma depletion layer (PDL) are observed. The 3D PIC simulation reveals the global views of the solar-wind magnetosphere interactions and the magnetic polar cusp structures.

Keywords: PIC, Magnetosphere, Mercury, CUSP, PDL

1. Introduction

Large-scale global three-dimensional PIC simulations have been performed in order to analyze the interaction between the solar-wind with the whole terrestrial magnetosphere as shown in Fig. 1. To our knowledge, this is the first simulation performed within the global 3D PIC view. Present analysis is first focused on the polar magnetic cusp region, more precisely on the dynamics of the cusp boundaries and particle entry area. The interplanetary magnetic field (IMF) is purely northward in order to identify more clearly the main cusp features to be compared with statistical 3-years Cluster observations. Present simulations are performed with a higher resolution, where one grid size equal to 0.2 Earth radii, as compared with our previous works [1-11]. Results show that different quantities need to be used in order to identify appropriately the cusp boundaries, for example, B_t (total magnetic field), $\text{Grad-}B_t$, ion density, ion flow, etc.. Main features of the cusp for northward IMF are characterized as follows: (i) a more draped B topology close to the outer boundary, (ii) a strong density peak within the cusp with multiple humps; this peak shifts poleward and disappears for high latitude, (iii) a strong peak in ion field aligned flow within the cusp, with a tailward (sunward) convection at low (high) latitude. A particular point is the evidence of a layer characterized by (a) a subAlfvénic/superAlfvénic ion flow transition, and (b) slow mode feature (increase of B, and decrease of N_i). Both features are in favor of the formation of PDL at the exterior cusp near a possible lobe reconnection

site in good agreement with experimental observations. In the present case, the location of this layer and of the reconnection site is slightly below latitude that evidenced in the statistics of Cluster data.

Statistical experimental observations of the cusp boundaries from Cluster mission made by [12] have clearly evidenced the presence of a transition layer inside the magnetosheath near the outer boundary of the cusp, This layer characterized by $\text{Log}(M_A) \sim 1$ allows a transition from super-Alfvénic to sub-Alfvénic bulk flow from the exterior to the interior side of the outer cusp and has been mainly observed experimentally as the interplanetary magnetic field (IMF) is northward. The role of this

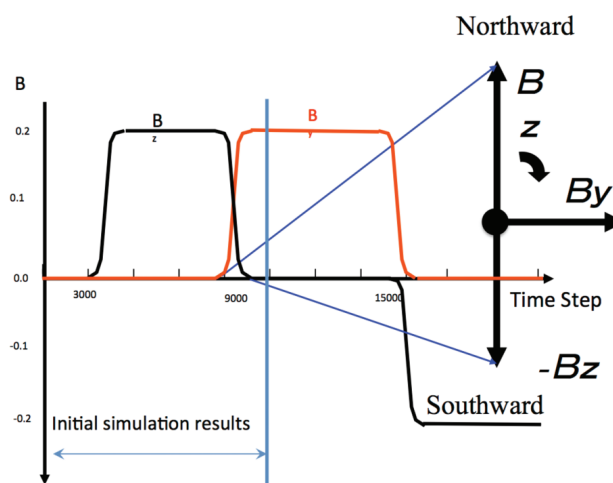


Fig. 1 Time sequence of IMF rotations from B_z to B_y .

layer is important in order to understand the flow variations and later the entry and precipitation of particles when penetrating the outer boundary of the cusp. Present results retrieve quite well the presence of this layer within the meridian plane for exactly northward IMF, but its location differs in the sense that it is located slightly below the X reconnection region associated to the nearby magnetopause (above the outer boundary of the cusp). In order to clarify this question, an extensive study has been performed by performing: a 3D mapping of this transition layer in order to analyze more precisely the possible spatial extension of this layer on the magnetosphere flanks.

2. 3D Global Simulation

In this section, we mainly discuss about main features of our simulations. The main advantages of present simulations are: (i) they are self-consistent simulations; (ii) the present simulation includes some kinetic effects although some attentions should be paid due to the limit size of grids; (iii) they are 3D simulations; and (iv) they are global. Therefore, some significant 3D fetures such as magnetic sashes, NENL (Near Earth Neutral Line) etc. can be included and we can self-consitently analyze how ions and electrons enter the magnetotail and where, when, and how they are energized. However, our global simulation also includes some limitations. For example, limited “space” resolution may exclude some effects such as: “thin” boundary layers, short wavelength instabilities etc.. These also may lead us to compromise on plasma parameters values. However, such limitations may be improved with the increase of computational ressources in the future.

The global MHD simulation can simulate properly the transport energy and momentum between different magnetospheric plasma regions despite their very large separation distances including the notion of magnetospheric convections, the general shape of magnetosphere, and their dependence on the incident solar wind conditions. Despite of these strong advantages, there still some questions remains because some evolutions of the global magnetospheric system may strongly depend on kinetic processes such as: (1) both precipitations and accelerations of both ions and electrons in the magnetic cusp region; and (2) transport of particles form the magnetic cusp to the plasma sheet. These strongly lead us to perform a 3D global electromagnetic full PIC simulation.

3. Simulation Results

In this section, we mainly discuss about main features of our simulations. As indicated in the time sequence of IMF rotation in Fig. 1, (a) the northward IMF has been applied after $t=3000$ and stay constant until $t=9000$; (b) the northward IMF gradually begin to rotate to dusk-dawn direction and stay constant until $t=15000$; and (c) finally rotate to southward and stay constant until 27000. The magnetic field configurations from IMF northward to southward are plotted in Fig. 2. Figure 2a is the

northward IMF case and the magneto-tail magnetic field closed at $x=-30\text{Re}$ and the magnetic field transit from the dipolar terrestrial to the tail magnetic field. As IMF rotates from north to dusk-dawn as shown in Fig. 2bc, the last closed dipolar field moves earthward from -30Re to -20Re . The magnetic sashes forms and rotates out to (Z, X) meridian plane. The stretching of the tail magnetic field occurs.

The southward IMF rotation can be decomposed into two sub-processes a and b as indicated in Fig. 2de. In sub-process a, the tail magnetic field stretches. The tail magnetic field progressively expands tailwards. In the sub-process b, tail magnetic field stops stretching. The abrupt transition between terrestrial and tail magnetic field occurs. The X-lines both at subsolar region and in the nearby tail at $x=-12\text{Re}$ are formed. A neutral ring evidenced in the equatorial plane connects both X-regions. Magnetic field lines adjacent the equatorward cusp boundary connected to the open magnetopause at low latitude [13]. Magnetosheath plasma enters magnetopause and populates the fields lines, thus, strong parallel precipitations of particles can be expected. With southward IMF, the IMF and terrestrial magnetic fields are antiparallel, and these two magnetic field may reconnect at the dayside magnetopause, and one expect the consequent transport and magnetic flux to the tail lobes causes increased magnetic stress in that region. This build up of magnetic flux leads to reconnection in the magnetotail. Here we will not mention anything about the reconnection processes themselves due to the present constraints of the simulation. For example, reconnections on the tail will be developed, but they may not be the ones that are commonly discussed kinetic ones in magnetospheric physics community. Here, we try to identify whether the global features in terms of magnetic field gradient,

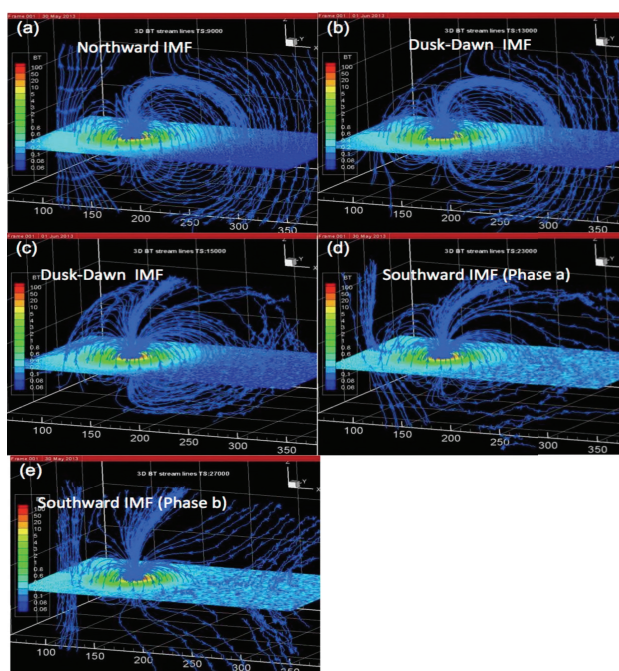


Fig. 2 Time sequence of magnetic field configurations in our simulation rotating IMF from north to south.

currents that are the ingredient necessary for magnetic substorm can be identified or not within this 3D PIC simulation approach.

We show the global view of magnetosphere of the northward IMF in 3D slicing in Fig. 3. A global view of the magnetosphere and the magnetic cusp structure can be observed. Asymmetric reconnection X-lines in the polar region and piles up of magnetic field in the dayside magnetosheath and high latitude polar region close to magnetic reconnection X lines also can be observed. This asymmetric structure can be better visualized showing 3D isosurface of $\text{Log}(M_A) \sim 1$ in Fig. 4. Due to the complicate 3D reconnecting flow, the part of $\text{Log}(M_A) \sim 1$ over the exterior cusps is strongly modified and move toward the earth. The complexity of the cusp makes the 3D analysis extremely difficult.

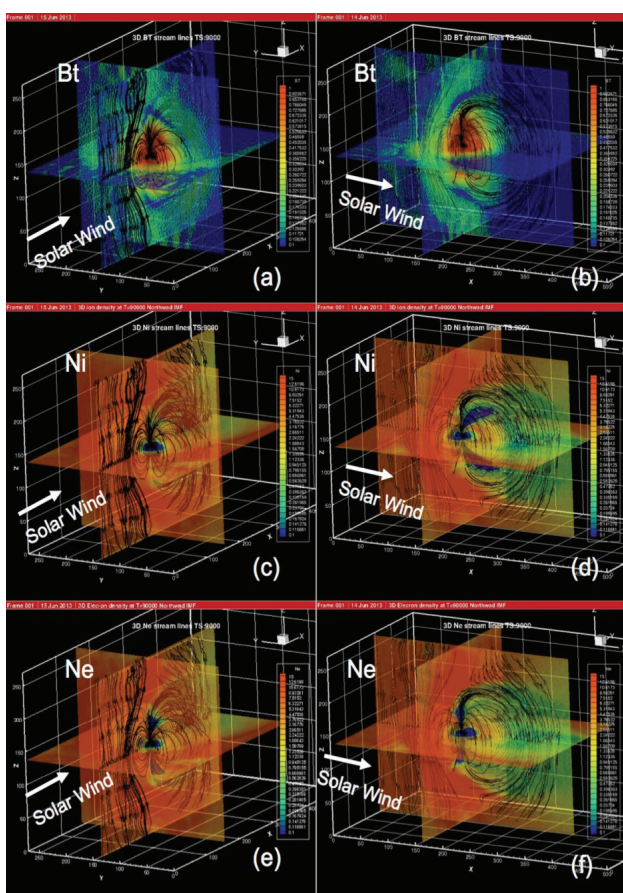


Fig. 3 3D global view of Bt, Ni, and Ne.

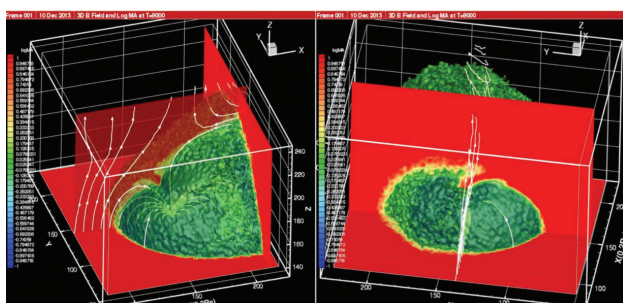


Fig. 4 Isosurface of $\text{Log}(M_A) \sim 1$ layer near the magnetic cusp region.

4. Conclusions

Although the size of our global simulation is limited and still small, the post process procedure to compare with the observational results is not well established, and the extent of the physical validity of the global PIC is not so clear, the global PIC simulation is still the powerful tool to analyze the global interaction between solar-wind and magnetosphere as we evidenced in the present paper. The comparative study with MHD and statistical studies of CLUSTER satellite observations shows many significant features such as SEC, FAB, PDL layers can be simulated and analyzed using the global PIC simulations. The advancement of computer power can resolve many limitations of the global PIC simulation such as the limited size in the simulation. However, at the same time, the post process procedure and data analysis technique to map the simulation data to real physics is also significant.

Acknowledgements

We would like to thank Dr. Tatsuki Ogino for his valuable advice and Dr. Ogino for encouragements. We would also like to thank Dr. Lavraud valuable comments on our research.

References

- [1] O. Buneman, *et al.*, “Solar wind-magnetosphere interaction as simulated by a 3-D EMparticle code,” *Plasma Science, IEEE Transactions on*, vol. 20, pp. 810-816, 1992.
- [2] D. Cai, *et al.*, “Magnetotail field topology in a three-dimensional global particle simulation,” *PLASMA PHYSICS AND CONTROLLED FUSION*, vol. 48, p. 123, 2006.
- [3] D. Cai, *et al.*, “Bifurcation and hysteresis of the magnetospheric structure with a varying southward IMF: Field topology and global three-dimensional full particle simulations,” *Journal of Geophysical Research: Space Physics*, vol. 114, 2009.
- [4] D. Cai, *et al.*, “Particle entry into the inner magnetosphere during duskward IMF By: Global three-dimensional electromagnetic full particle simulations,” *Geophysical research letters*, vol. 33, 2006.
- [5] D. S. Cai, *et al.*, “Visualization and criticality of three-dimensional magnetic field topology in the magnetotail,” *Earth Planets Space*, vol. 53, p. 1011, 2001.
- [6] B. Lembege, *et al.*, “Signatures of substorm triggering in the magnetotail during IMF,” 2008.
- [7] K.-I. Nishikawa and S.-i. Ohtani, “Global particle simulation for a space weather model: Present and future,” *Plasma Science, IEEE Transactions on*, vol. 28, pp. 1991-2006, 2000.
- [8] K. I. Nishikawa, “Particle entry into the magnetosphere with a southward interplanetary magnetic field studied by a three-dimensional electromagnetic particle code,”

- Journal of Geophysical Research-Space Physics*, vol. 102, pp. 17631-17641, 1997.
- [9] K. I. Nishikawa and S. Ohtani, "Global particle simulation for a Space Weather Model: Present and future," *IEEE Transactions on Plasma Science*, vol. 28, pp. 1991-2006, 2000.
- [10] K. I. Nishikawa and S. Ohtani, "Evolution of thin current sheet with a southward interplanetary magnetic field studied by a three-dimensional electromagnetic particle code," *Journal of Geophysical Research-Space Physics*, vol. 105, pp. 13017-13028, 2000.
- [11] K. I. Nishikawa and S. Ohtani, "Particle simulation study of substorm triggering with a southward IMF," *Dynamic Processes in the Critical Magnetospheric Regions and Radiation Belt Models, Proceedings*, vol. 30, pp. 2675-2681, 2002.
- [12] B. Lavraud, *et al.*, "Cluster observations of the exterior cusp and its surrounding boundaries under northward IMF," *Geophysical research letters*, vol. 29, pp. 56-1-56-4, 2002.
- [13] M. Lockwood and M. Smith, "Low and middle altitude cusp particle signatures for general magnetopause reconnection rate variations: 1. Theory," *Journal of Geophysical Research: Space Physics*, vol. 99, pp. 8531-8553, 1994.

水星探査計画「Bepi Colombo」のための大域的 3 次元電磁粒子シミュレーションを用いた水星磁気圏シミュレータの開発

課題責任者

蔡 東生 筑波大学 システム情報系

著者

蔡 東生 筑波大学 システム情報系

本研究では、2016 年打ち上げの予定の水星探査衛星「Bepi-Colombo」の観測結果をデータアシミレートするための大域的 3 次元電磁粒子シミュレーションを行う。シミュレーションの正当性、適用可能範囲を調べるため、最初に衛星 4 基で観測している Cluster 衛星の統計的観測結果との比較をカスプ領域を中心に行った。その結果、カスプ領域の境界である、磁気シースとの境界の Plasma Depletion Layer、磁尾部境界の磁気再結合ジェット、外部カスプの半磁性流を確認した。また、アルフベンマッハ速度が亜アルフベンマッハ速度に遷移する境界を詳しく調べることにより、3 次元的なカスプ形状を詳しく調査した。これらにより、水星探査における、3 次元粒子コードの有用性を確認した。

キーワード: 粒子コード, 水星, ベッピコロンボ, カスプ, プラズマ排出領域

